

A record-high trapped field of 1.61 T in MgB₂ bulk comprised of copper plates and soft iron yoke cylinder using pulsed-field magnetization

Tatsuya Hirano , Yuhei Takahashi, Sora Namba , Tomoyuki Naito  and Hiroyuki Fujishiro 

Department of Physical Science and Materials Engineering, Faculty of Science and Engineering, Iwate University, Morioka 020-8551, Japan

E-mail: fujishiro@iwate-u.ac.jp and thirano1995@gmail.com

Received 10 March 2020, revised 3 May 2020

Accepted for publication 21 May 2020

Published 18 June 2020



Abstract

A trapped field of $B_T = 1.61$ T was experimentally achieved at the central surface of an MgB₂ bulk composite (60 mm in diameter and 20 mm in height) at 20 K by double pulsed-field magnetization (PFM) using a split-type coil. The composite bulks consisted of two MgB₂ ring bulks sandwiched by thin copper ring plates, which were then stacked, and a soft iron yoke cylinder was inserted in the central bore of the rings. The copper ring plates delayed the rise time and duration of the magnetic pulse due to eddy currents. The inserted soft iron yoke attracted the magnetic flux and enhanced the trapped field strength mainly due to its large permeability. As a result, the trapped field was enhanced from $B_T = 0.34$ T for the single MgB₂ ring bulk without the copper plates and soft iron yoke to $B_T = 1.00$ T for the composite with both copper plates and the soft iron yoke. The inserted soft iron yoke can be exploited to enhance the trapped field because the intrinsic B_T of the single MgB₂ ring bulk was smaller than the saturation field of the yoke (~ 2 T). Using an optimized second pulse application after suitable flux trapping from the first pulse application, the trapped field was enhanced considerably to $B_T(2nd) = 1.61$ T, which is a record-high trapped field for an MgB₂ bulk by PFM to date. The combination of the longer magnetic pulse application by the copper plates, the enhancement of the effective applied field by the inserted soft iron yoke, and the double pulse application using split-type coil is an effective technique to enhance the trapped field in the MgB₂ bulk using PFM.

Keywords: MgB₂, pulsed field magnetization, trapped field, soft iron yoke cylinder, double pulse application, copper plate stack, rise time elongation

(Some figures may appear in colour only in the online journal)

1. Introduction

Large, single-grain RE-Ba-Cu-O (REBaCuO, RE: a rare earth element or Y) bulk superconductors can trap higher magnetic field by strong vortex pinning effect and are a promising material for use as a compact, high-strength trapped field magnet (TFM) [1] for various practical applications, such as rotating machines, magnetic separation, flywheel energy storage

systems and compact cryogen-free nuclear magnetic resonance (NMR) and magnetic resonance imaging (MRI) systems [2–6]. A record high trapped field of $B_T(\text{FCM}) = 17.6$ T at 26 K has been achieved in the GdBaCuO disk bulk pair activated by field-cooled magnetization (FCM) [7, 8]. During FCM, the bulk is cooled below the transition temperature, $T_c = 92$ K, under the applied field, B_{ex} , using superconducting magnet (SM) and then the magnetic field decreases to zero.

On the other hand, MgB₂ bulk superconductors have also promising potential as TFMs, such as being rare-earth-free, lightweight and presenting a homogeneous trapped field distribution [9], which are in clear contrast with REBaCuO bulks. The better and larger MgB₂ polycrystalline TFMs can be realized because of their long coherence length, ξ , below $T_c = 39$ K [10]. MgB₂ bulks with high critical current density, J_c , have been fabricated by various methods and usually activated by FCM [11–15]. A record-high trapped field of $B_T(\text{FCM}) = 5.4$ T has been achieved at 12 K on a surface of a MgB₂ disk bulk 20 mm in diameter [16]. In this way, FCM can achieve the maximum trapped field of the bulk. However, since the SM is expensive and heavy, FCM is generally ill-suited for wide practical applications.

Pulsed-field magnetization (PFM) is another magnetizing method to magnetize bulk superconductors [17–21], which is mobile, inexpensive experimental setup with no use of SM. During PFM, the bulk is cooled below T_c , and the magnetic pulsed field with the rise time of milliseconds is applied using a copper coil and condenser bank. However, the trapped field by PFM, $B_T(\text{PFM})$, is generally lower than that by FCM because of a large temperature rise caused by the dynamics of the magnetic flux during the magnetic pulse application [22].

Multi-pulse techniques are effective to enhance the B_T value for REBaCuO bulks due to the reduction of the temperature rise [23–26]. We have achieved the trapped field of $B_T(\text{PFM}) = 5.20$ T on a GdBaCuO bulk 45 mm in diameter at 29 K using a modified multi-pulse technique with stepwise cooling (MMPSC) [17], which is a record-high $B_T(\text{PFM})$ for REBaCuO bulk by PFM to date. The PFM technique has also been applied to MgB₂ bulks [27–32]. $B_T(\text{PFM}) = 0.81$ T was achieved at 14 K for a high- J_c MgB₂ bulk fabricated by the hot isostatic pressing (HIP) method magnetized using a copper solenoid coil, in which $B_T(\text{FCM}) = 2.23$ T was trapped at 16 K by FCM [29]. However, flux jumps took place frequently during PFM in the high- J_c MgB₂ bulks and consequently the final $B_T(\text{PFM})$ value decreased for larger pulsed fields. The multi-pulse application would be to enhance the trapped field for the MgB₂ bulk.

The effectiveness of the split-type coil (or vortex-type coil) during PFM has been clarified for REBaCuO bulks experimentally [33, 34] and numerically [19, 35]. The magnetic flux starts to intrude not from the periphery, but mainly from the both surfaces of the disk bulk, and is trapped in the center of the bulk, even for lower pulsed fields. It was shown that the maximum B_T could be enhanced in comparison to that obtained using the solenoid-type coil. In this case, the temperature rise during PFM for the split-type coil was smaller than that for the solenoid-type coil. We have achieved a trapped field of $B_T(\text{PFM}) = 1.1$ T on a high- J_c MgB₂ bulk at 13 K without flux jumps by PFM using a split-type coil, in which a pair of soft iron yokes were inserted in the bore of the split-type coil. $B_T(\text{PFM}) = 1.1$ T has been the record high trapped field by PFM for MgB₂ bulk since 2016 [36]. We have performed many PFM experiments and numerical simulations for REBaCuO and MgB₂ bulks, in which the following effectiveness has been suggested to enhance the trapped field; the use of split-type coil [19, 33–35], the multi-pulse application for

the REBaCuO bulk [17, 23, 24], the use of soft iron yoke in the pulse coil [19] and the long pulse application [37].

In this study, we have investigated the trapped field properties of MgB₂ ring bulk composites inserted by soft iron yoke at 20 K by single and double pulsed field applications using a split-type coil. Furthermore, the effect of thin copper plates, which sandwiched the MgB₂ ring bulks, was investigated to expect the longer magnetic pulse application. As a result, a new record-high trapped field of $B_T = 1.61$ T was experimentally achieved at 20 K for an MgB₂ ring bulk comprised of both copper plates and a soft iron yoke using double pulsed-field application by split-type coil.

2. Experimental details

We performed the PFM experiments using three types of bulk modules. An MgB₂ ring bulk (20 mm in inner diameter (I.D.), 60 mm in outer diameter (O.D.) and 19 mm in height (H)) was fabricated by an *in-situ* infiltration method [38], in which $B_T(\text{FCM}) = 1.57$ T was trapped by FCM at 20 K. We abbreviate this as ‘single bulk’, as shown in figure 1(a). The single bulk was sliced in half ($H = 9$ mm), and each ring bulk was sandwiched by oxygen-free copper plates 0.5 mm in thickness using Apiezon-NTM grease, and then stacked, as shown in figure 1(b). We abbreviate this as ‘composite (w/o yoke)’. A soft iron yoke cylinder (20 mm in diameter and 20 mm in H) was inserted in the composite (w/o yoke), as shown in figure 1(c). We abbreviate this as ‘composite (w/yoke)’.

Figure 2 shows the experimental setup for PFM using the split-type coil. Each MgB₂ bulk module was fastened in a brass holder using a stainless steel (SS) bolt and nut with thin indium foil and connected to the cold stage of a Gifford–McMahon (GM) cycle helium refrigerator in a vacuum chamber. In the previous study, a copper holder was used to fasten the disk bulk for the split-type coil [19], in which non-negligible temperature rise was observed due to the eddy current flowing in the holder during PFM. To eliminate the temperature rise in the holder, a brass holder was used in this study, which has lower electrical conductivity. A Hall sensor (HG-106 C; ASAHI KASEI) was placed to the center of the bulk surface, and a thermometer (CernoxTM) was connected to the brass holder. The split-type coil (72 mm in I.D., 124 mm in O.D., 35 mm in H), which was submerged in liquid nitrogen, was placed outside the vacuum chamber, in which a pair of Ni-plated soft iron yokes (60 mm in diameter and 65 mm in height) was inserted in the central bores of the coil.

The strength of the magnetic pulse was estimated using the following methods. Figure 3 shows the experimental method to estimate the magnitude of pulsed field, $B_{\text{ex}}(\text{shunt})$ and $B_{\text{ex}}(\text{Hall})$. The time evolution of magnetic field, $B_{\text{ex}}(\text{shunt})(t)$, was estimated by observing the current, $I(t)$, flowing through the shunt resistor from the pulse current source (condenser bank) using a digital oscilloscope (YOKOGAWA Electric, DL1640). For example, to achieve $B_{\text{ex}}(\text{shunt})^{\text{max}} = 1.5$ T at the center of the split coil at $T_s = 40$ K ($>T_c$ of the MgB₂ bulk), $I_{\text{peak}} = 440$ A. The time evolution of the magnetic field, $B_{\text{ex}}(\text{Hall})(t)$, was also simultaneously monitored at the central

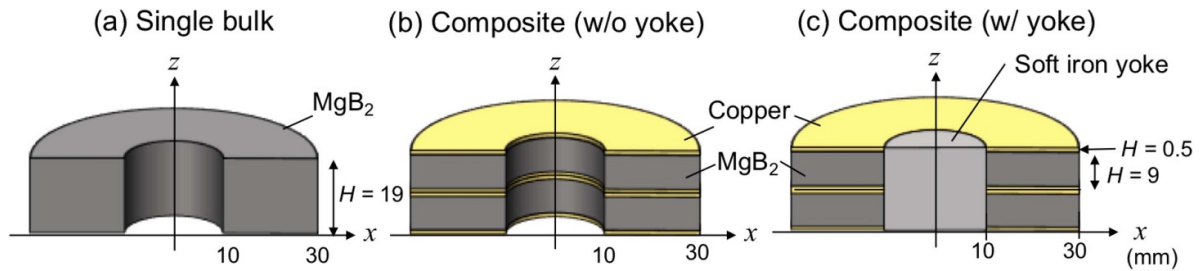


Figure 1. Three types of MgB_2 bulk modules used for the PFM experiments: (a) ‘single bulk’, (b) ‘composite (w/o yoke)’, where two sliced ring bulks were sandwiched by oxygen-free copper plates and are stacked, and (c) ‘composite (w/yoke)’, where a soft iron yoke cylinder is inserted in (b).

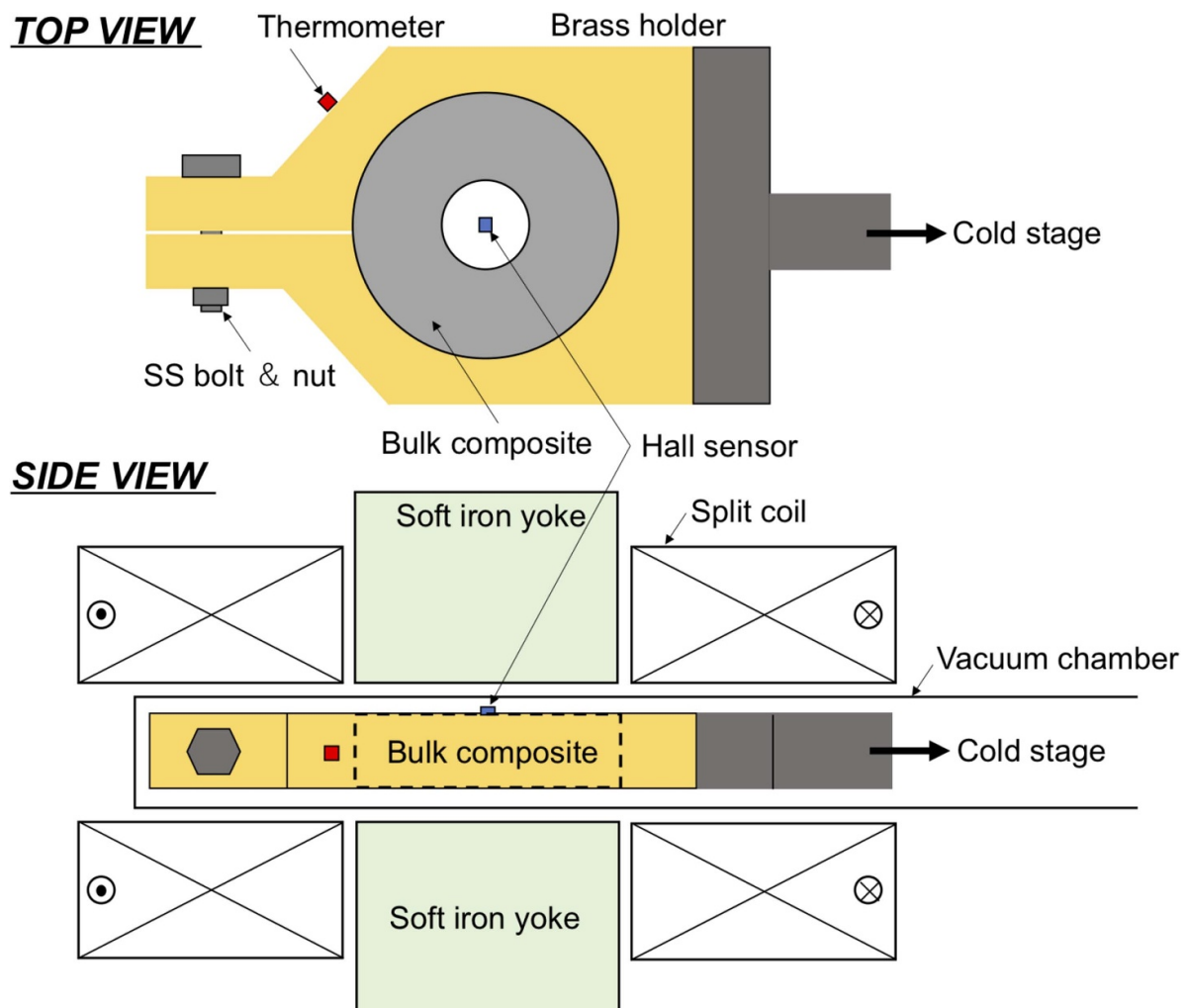


Figure 2. Experimental setup of the PFM for the three types of bulk modules using split-type coil with soft iron yoke.

surface of the single MgB_2 ring bulk and the composite (w/o yoke) by measuring the Hall voltage of the Hall sensor using the digital oscilloscope. For the composite (w/yoke), the time evolution of magnetic field, $B_{\text{ex}}(\text{Hall})(t)$, which is defined as $B_{\text{ex}}(\text{yoke})(t)$ hereafter, was monitored by measuring the Hall voltage at the central surface of the soft iron yoke.

The initial temperature, T_s , of the bulk was set to 20 K, and a single magnetic pulse, $B_{\text{ex}}(\text{Hall})(t)$, with a peak up to 2.0 T was applied via a pulsed current flowing in the coil, as shown in

figure 4(a). The PFM experiments were also performed using double pulse application, as shown in figure 4(b). The first pulse of $B_{\text{ex1}}(\text{Hall})^{\text{max}} = 1.20$ or 1.32 T was applied at 20 K. Next, once the temperature of the bulk returned to 20 K, the second pulse, $B_{\text{ex2}}(\text{Hall})^{\text{max}}$, ranging from 1.1 to 1.6 T, was applied to the bulk.

During PFM, the time evolution of the temperature, $T(t)$, and the trapped field, B_T , which was defined as the final value of $B_T(t)$ at 500 ms, were measured. After the removal of the

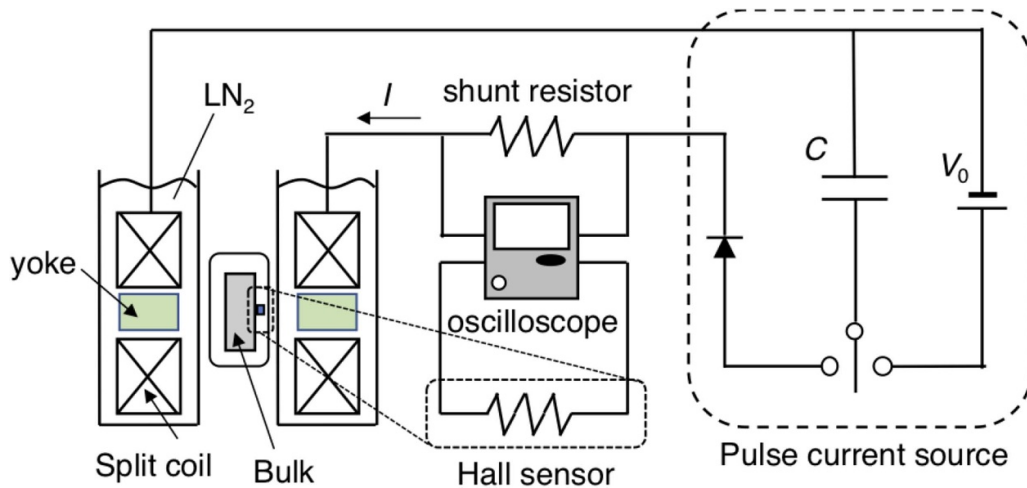


Figure 3. The experimental method to estimate the magnitude of pulsed field, $B_{\text{ex}}(\text{shunt})$ and $B_{\text{ex}}(\text{Hall})$.

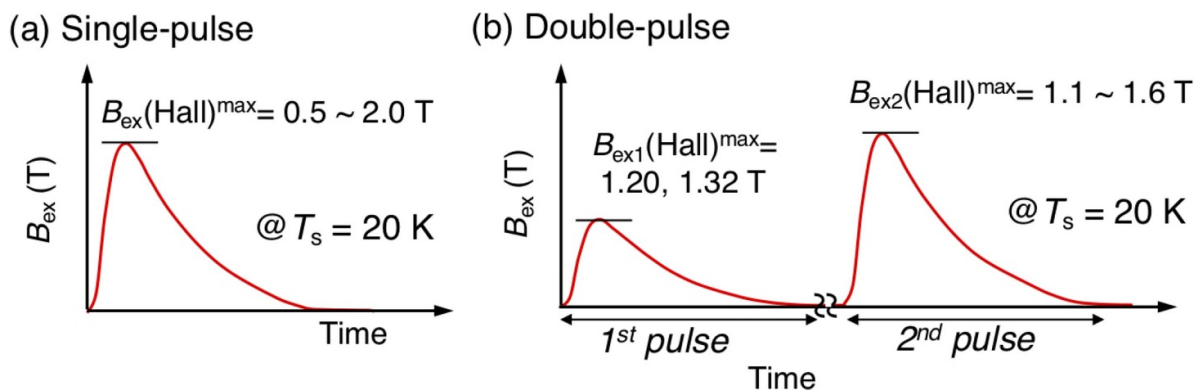


Figure 4. Schematic illustration of (a) single-pulse and (b) double-pulse application during PFM at $T_s = 20$ K.

split-type coil (15 min after the each pulse application), two-dimensional trapped field profiles were mapped at 5 mm above the bulk surface (on the outer surface of the vacuum chamber) by scanning a Hall sensor (BHA 921; F W Bell) using an x - y stage controller.

3. Results and discussion

3.1. Effect of the copper plates and soft iron yoke

First, we clarify the effects of the copper plate stack and soft iron yoke insertion on the magnetic pulse, $B_{\text{ex}}(t)$. Figure 5(a) shows the time dependence of $B_{\text{ex}}(\text{shunt})(t)$ for an applied magnetic field of 1.03 T, which was measured for the ‘single bulk’ case at $T_s = 40$ K. The rise time, t_{rise} , was about 20 ms, and the pulse duration was about 400 ms, which were determined by the coil inductance and the existence of the ferromagnetic soft iron yoke inserted in the bore of the split-type coil. In the figure, the $B_{\text{ex}}(\text{Hall})(t)$ profiles for the single bulk, composite (w/o yoke) and composite (w/yoke) cases are also shown, which were measured by the adhered Hall sensors. $B_{\text{ex}}(\text{Hall})(t)$ for the single bulk was slightly delayed, compared with $B_{\text{ex}}(\text{shunt})(t)$. However, the magnitude, rise time and duration of $B_{\text{ex}}(\text{Hall})(t)$ for the composites (w/o yoke) and

(w/yoke) cases are quite different with those for the single bulk case.

Figure 5(b) shows the relationship between the maximum values ($B_{\text{ex}}(\text{Hall})^{\text{max}}$ and $B_{\text{ex}}(\text{shunt})^{\text{max}}$) of the curves $B_{\text{ex}}(\text{Hall})(t)$ and $B_{\text{ex}}(\text{shunt})(t)$ for each case at $T_s = 40$ K. The maximum value of the $B_{\text{ex}}(\text{Hall})(t)$ curve, named as $B_{\text{ex}}(\text{Hall})^{\text{max}}$ for the composite (w/o yoke) was about 20% smaller than that of the $B_{\text{ex}}(\text{shunt})(t)$, named as $B_{\text{ex}}(\text{shunt})^{\text{max}}$, because of eddy currents flowing in the high-conductive copper plates along the direction to avoid the magnetic flux intrusion. On the other hand, the $B_{\text{ex}}(\text{Hall})^{\text{max}}$ value for the composite (w/yoke) was much larger than $B_{\text{ex}}(\text{shunt})^{\text{max}}$, and its rate increases with increasing $B_{\text{ex}}(\text{shunt})^{\text{max}}$. The $B_{\text{ex}}(\text{Hall})^{\text{max}}$ enhancement for the composite (w/yoke) mainly results from flux concentration in the ferromagnetic yoke cylinder, although the induced current flowing in the yoke acts to reduce the flux intrusion.

Figure 5(c) shows the rise time, $t_{\text{rise}}(\text{Hall})$, measured by the Hall sensor and $t_{\text{rise}}(\text{shunt})$, as a function of $B_{\text{ex}}(\text{shunt})^{\text{max}}$ at $T_s = 40$ K. The magnitude of $t_{\text{rise}}(\text{Hall})$ for the composite (w/o yoke) increased due to the copper plates, and that for the composite (w/yoke) increased more due to the existence of the yoke, compared with that for the single bulk. The detailed study using the copper plates is planned in the next paper.

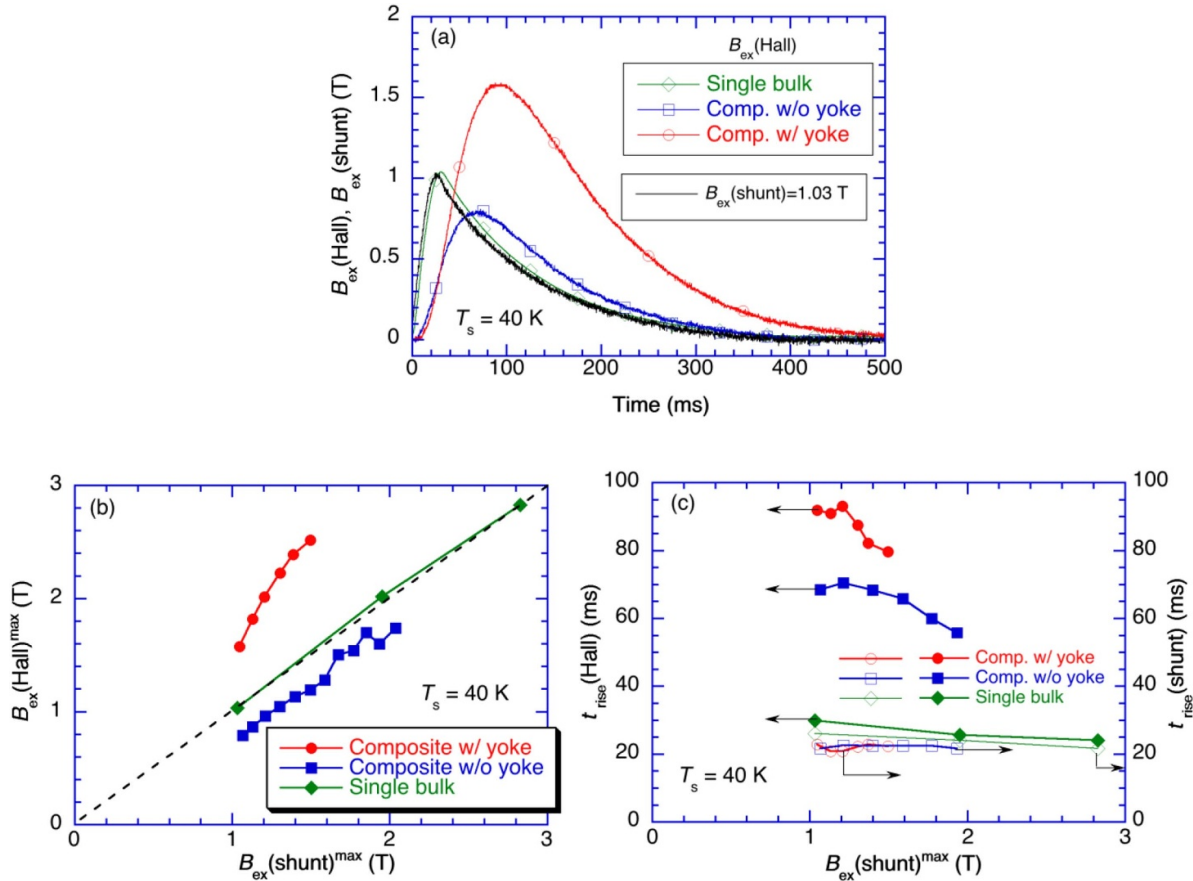


Figure 5. (a) The time dependence of $B_{\text{ex}}(\text{shunt})(t)$ for an applied magnetic field of 1.03 T, measured for the single MgB_2 bulk case, and $B_{\text{ex}}(\text{Hall})(t)$ for the single bulk, composite (w/o yoke) and composite (w/yoke) cases at $T_s = 40 \text{ K}$. (b) The relationship between the maximum values ($B_{\text{ex}}(\text{Hall})^{\text{max}}$ and $B_{\text{ex}}(\text{shunt})^{\text{max}}$) of the curves $B_{\text{ex}}(\text{shunt})(t)$ and $B_{\text{ex}}(\text{Hall})(t)$ for each case at $T_s = 40 \text{ K}$. (c) The rise time, $t_{\text{rise}}(\text{Hall})$ and $t_{\text{rise}}(\text{shunt})$, as a function of $B_{\text{ex}}(\text{shunt})^{\text{max}}$ at $T_s = 40 \text{ K}$.

3.2. Results for single pulse application

The PFM experiments were performed for the three types of MgB_2 modules at $T_s = 20 \text{ K}$ ($< T_c$ of the MgB_2 bulk). Figure 6 shows the trapped field, B_T , which is defined as the steady value of the curves $B_T(t)$ at $t = 500 \text{ ms}$, at the central surface of each MgB_2 module, as a function of $B_{\text{ex}}(\text{Hall})^{\text{max}}$ at 20 K. The trapped field profiles for each case, when the maximum B_T value was achieved, are also shown. For the single MgB_2 bulk case, the magnetic flux started to penetrate into the center at $B_{\text{ex}}(\text{Hall})^{\text{max}} = 0.85 \text{ T}$, and a maximum of $B_T = 0.34 \text{ T}$ was trapped at the central surface. For larger $B_{\text{ex}}(\text{Hall})^{\text{max}}$, the B_T value decreased due to a larger temperature rise. The trapped field profile is shown, for which a trapezoidal profile was measured 5 mm above the bulk surface. For the composite (w/o yoke), the magnetic flux started to penetrate into the center at $B_{\text{ex}}(\text{Hall})^{\text{max}} = 1.23 \text{ T}$, and then decreased with increasing $B_{\text{ex}}(\text{Hall})^{\text{max}}$. A maximum $B_T = 0.44 \text{ T}$ was trapped at the central surface. The $B_{\text{ex}}(\text{Hall})^{\text{max}}$ value for the composite (w/o yoke), at which the B_T value took a maximum, was larger than that for the single MgB_2 bulk. Here, a larger magnetic pulse is necessary to trap the magnetic flux at the center due to the existence of the copper plates, as shown in figure 5(b). The maximum B_T value for the composite (w/o

yoke) was slightly larger than that for the single bulk case. For the composite (w/yoke), the magnetic flux started to penetrate into the center around $B_{\text{ex}}(\text{Hall})^{\text{max}} = 1.03 \text{ T}$, took a maximum of $B_T = 1.00 \text{ T}$ at $B_{\text{ex}}(\text{Hall})^{\text{max}} = 1.20 \text{ T}$, and then decreased with increasing $B_{\text{ex}}(\text{Hall})^{\text{max}}$. It should be noted that for the composite (w/yoke), the B_T value was enhanced, but the $B_{\text{ex}}(\text{Hall})^{\text{max}}$ value at which B_T value took a maximum was nearly the same as that for the composite (w/o yoke). These results suggest that the enhancement of the B_T value resulted mainly from the yoke cylinder and that the $B_{\text{ex}}(\text{Hall})^{\text{max}}$ value at which B_T value takes a maximum was mainly determined by the copper plates, although we did not perform PFM experiments for the MgB_2 bulk with only the yoke without the copper plates.

Figure 7(a) shows the maximum temperature rise, T_{max} , during PFM for each composite, as a function of $B_{\text{ex}}(\text{Hall})^{\text{max}}$ at 20 K. For the single bulk, T_{max} abruptly increases at $B_{\text{ex}}(\text{Hall})^{\text{max}} = 0.85 \text{ T}$ due to the pinning loss of the flux trap [39], at which the magnetic flux reached the center of the bulk, and $B_T = 0.34 \text{ T}$ was trapped. T_{max} increased with increasing $B_{\text{ex}}(\text{Hall})^{\text{max}}$ due to the viscous loss of the flux movement [39]. For the composites (w/yoke) and (w/o yoke) cases, T_{max} linearly increased with increasing $B_{\text{ex}}(\text{Hall})^{\text{max}}$, even though the magnetic flux was not trapped the center of the bulk for

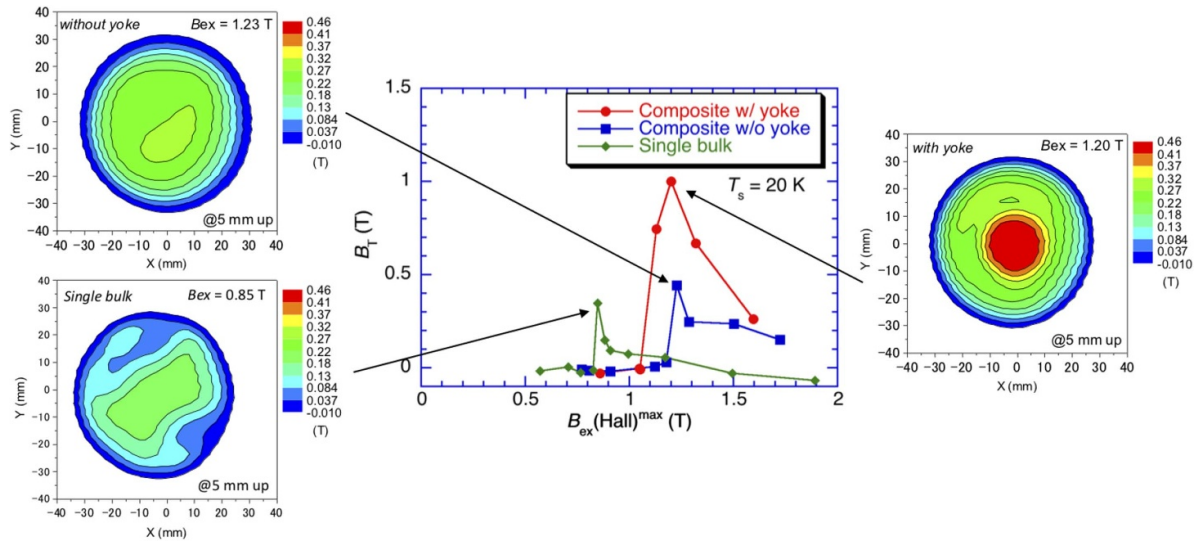


Figure 6. The trapped field, B_T , at the central surface of each module, as a function of $B_{\text{ex}}(\text{Hall})^{\text{max}}$ at 20 K. The trapped field profiles for each case, when the maximum B_T value was achieved, are also shown.

$B_{\text{ex}}(\text{Hall})^{\text{max}} < 1.2$ T. These results indicate that the heat generation took place mainly in the copper plates due to the eddy currents in addition to the heat generation due to the flux trap. For $B_{\text{ex}}(\text{Hall})^{\text{max}} > 1.2$ T, for which the magnetic flux was trapped, the temperature rise due to the flux trap was superimposed and T_{max} was larger than that of the single bulk. Because of the additional heat generation from the eddy current in the inserted yoke, the temperature rise of the composite (w/yoke) was larger than that of the composite (w/o yoke) for higher $B_{\text{ex}}(\text{Hall})^{\text{max}}$.

Figure 7(b) shows an example of the time dependence of the temperature, $T(t)$, in the composite (w/o yoke) for $B_{\text{ex}}(\text{Hall})^{\text{max}} = 0.91, 1.23$ and 1.29 T, which was measured on the surface of the brass holder. $T(t)$ took a maximum at $t = 2 \sim 3$ s and then linearly decreased with increasing time. The maximum temperature increased with increasing $B_{\text{ex}}(\text{Hall})^{\text{max}}$. Similar trends were also observed for other cases. The results in figure 7 reflect indirectly the trapped field properties during PFM, even though the thermometer was not adhered directly on the bulk surface.

Figure 8 shows the time dependence of the applied field, $B_{\text{ex}}(t)$, and the trapped field, $B_T(t)$, for each case and for each single pulse application of $B_{\text{ex}}(\text{Hall})^{\text{max}}$. Figures 8(a) to (c) show the results for the single MgB_2 ring bulk, where $B_{\text{ex}}(\text{shunt})(t)$ and $B_{\text{ex}}(\text{Hall})(t)$ are also shown. The magnetic flux cannot penetrate well to the center of the bulk due to its magnetic shielding for $B_{\text{ex}}(\text{Hall})^{\text{max}} = 0.83$ T (figure 8(a)). With increasing $B_{\text{ex}}(\text{Hall})^{\text{max}}$, the magnetic flux was able to penetrate into the center, and the $B_T(t = 500 \text{ ms})$ value took a maximum at $B_{\text{ex}}(\text{Hall})^{\text{max}} = 0.85$ T (figure 8(b)). For $B_{\text{ex}}(\text{Hall})^{\text{max}} = 0.88$ T, the $B_T(t = 500 \text{ ms})$ value decreased due to a large flux flow out of the bulk (figure 8(c)). Figures 8(d) to (f) show the results for the composite (w/o yoke). Here, similar trends to the single bulk were observed. The B_T value took a maximum of $B_T = 0.42$ T at $B_{\text{ex}}(\text{Hall})^{\text{max}} = 1.23$ T (figure 8(e)), and then decreased at $B_{\text{ex}}(\text{Hall})^{\text{max}} = 1.30$ T. For

higher $B_{\text{ex}}(\text{Hall})^{\text{max}}$, as shown in figure 8(f), a long gradual decay in $B_T(t)$ can be seen at $100 \text{ ms} < t < 250 \text{ ms}$. This is a characteristic decay in MgB_2 bulk during PFM [30], which was also reported by other researcher [32], but has not been clarified the reason. Figures 8(g) to (i) show the results for the composite (w/yoke), where $B_{\text{ex}}(\text{yoke})(t)$ is also shown, in addition to $B_{\text{ex}}(\text{shunt})(t)$ and $B_{\text{ex}}(\text{Hall})(t)$. The B_T value took a maximum of 1.00 T at $B_{\text{ex}}(\text{Hall})^{\text{max}} = 1.21$ T (figure 8(h)) and then decreased at $B_{\text{ex}}(\text{Hall})^{\text{max}} = 1.32$ T. The trapped field of the composite (w/yoke) was higher than that of the composite (w/o yoke), because the iron yoke has a large permeability. The period of the characteristic $B_T(t)$ decay for the composite (w/yoke) becomes longer at $150 \text{ ms} < t < 400 \text{ ms}$. These results indicate that the composite bulk is considered to be pseudo-long pulsed field magnetization technique.

3.3. Results for double pulse application

In the previous subsection, the effects of the copper plates on the MgB_2 bulk surface and the insertion of soft iron yoke cylinder on the trapped field enhancement were clearly confirmed for the single pulse application. In this subsection, the effect of the double pulse application is presented. Figure 9(a) shows the trapped field, $B_T(2\text{nd})$, on the central surface of the composite (w/yoke) at $T_s = 20$ K, as a function of the second applied pulsed field, $B_{\text{ex}2}(\text{Hall})^{\text{max}}$, after the first pulsed field, $B_{\text{ex}1}(\text{Hall})^{\text{max}}$, of 1.20 T or 1.32 T was applied and the magnetic flux was already trapped. After the application of $B_{\text{ex}1}(\text{Hall})^{\text{max}} = 1.32$ T, the final $B_T(2\text{nd})$ value was 0.65 T, as shown in figure 8(i). For the second pulse application, $B_T(2\text{nd})$ sharply increased, took a maximum of 1.61 T at $B_{\text{ex}2}(\text{Hall})^{\text{max}} = 1.26$ T, and then decreased with increasing $B_{\text{ex}2}(\text{Hall})^{\text{max}}$. The $B_T(2\text{nd}) = 1.61$ T is a record high B_T value for an MgB_2 bulk by PFM to date. The trapped field profile 5 mm above the bulk surface was fairly

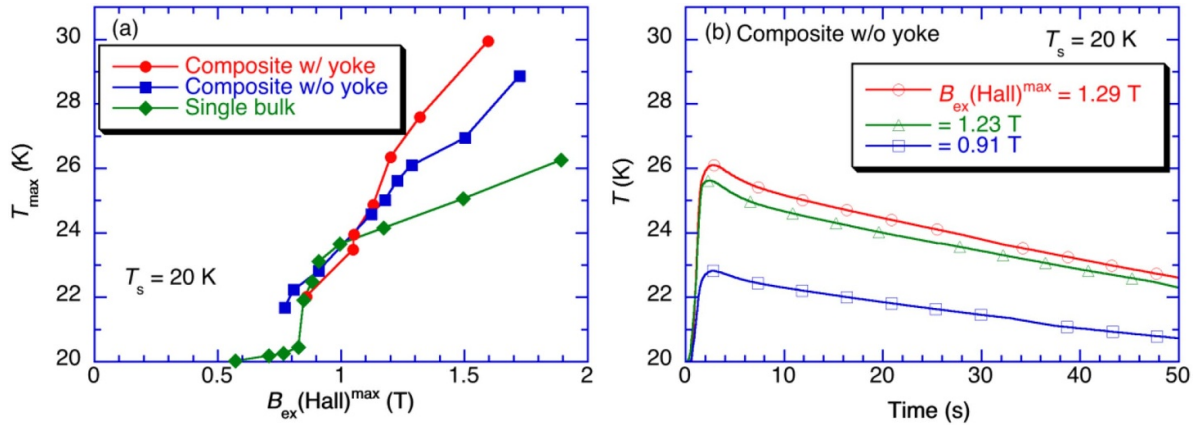


Figure 7. The maximum temperature rise, T_{\max} , during PFM for each composite, as a function of $B_{\text{ex}}(\text{Hall})^{\max}$ at 20 K. (b) An example of the time dependence of the temperature, $T(t)$, for the composite (w/o yoke) for $B_{\text{ex}}(\text{Hall})^{\max} = 0.91, 1.23$ and 1.29 T at 20 K.

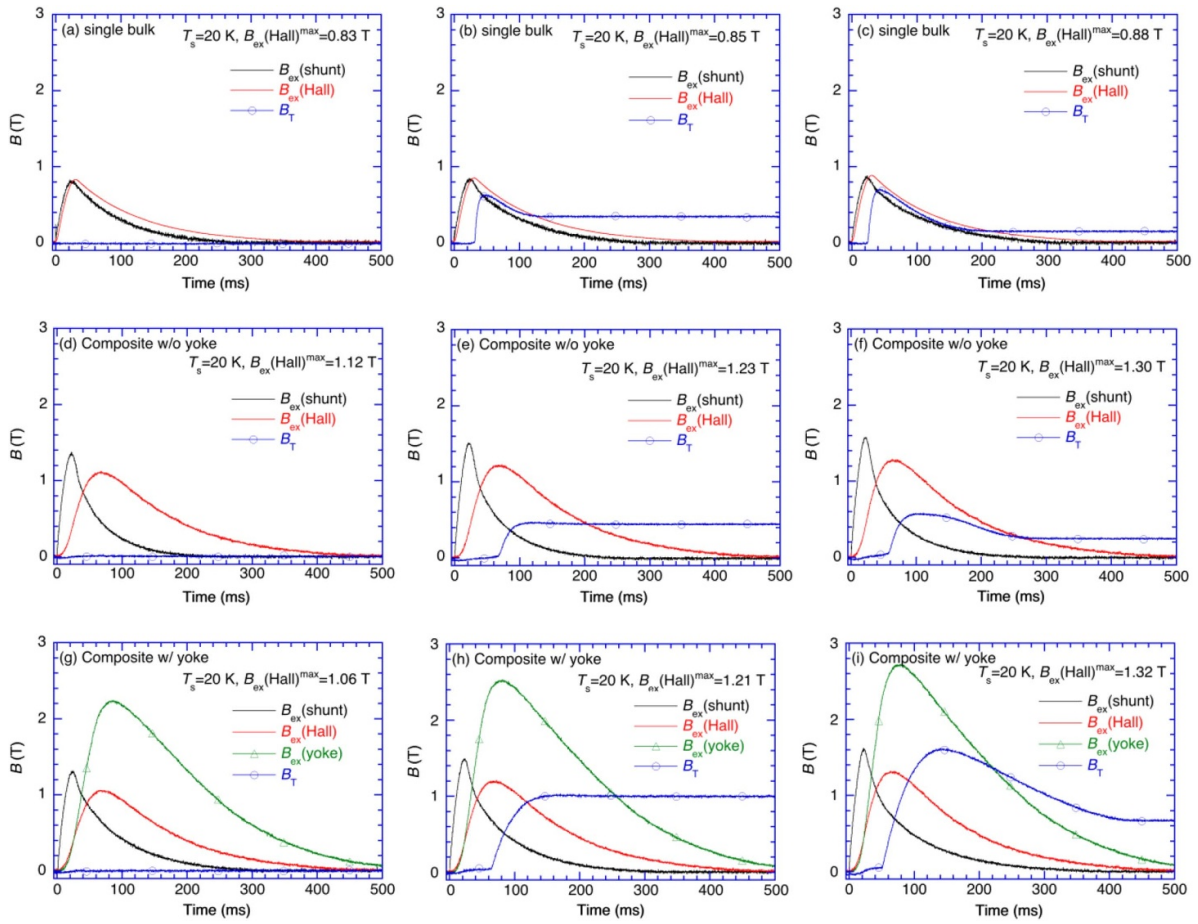


Figure 8. The time dependence of the applied fields, $B_{\text{ex}}(t)$, and the trapped field, $B_{\text{T}}(t)$, for single pulse application of $B_{\text{ex}}(\text{Hall})^{\max}$ for (a)–(c) the single bulk, (d)–(f) the composite (w/o yoke), and (g)–(i) the composite (w/yoke).

cone shaped. The highest B_{T} value comes from the reduction of temperature rise due to the already trapped magnetic flux during the 1st magnetic pulse [17, 40]. For the case of $B_{\text{ex}1}(\text{Hall})^{\max} = 1.20$ T, similar $B_{\text{T}}(2\text{nd})$ vs $B_{\text{ex}2}(\text{Hall})^{\max}$ behavior can be observed. However, the maximum $B_{\text{T}}(2\text{nd})$ value was smaller than that for $B_{\text{ex}1}(\text{Hall})^{\max} = 1.32$ T. These results suggest that an optimum trapped field and $B_{\text{T}}(1\text{st})$ profile

exists to maximize the $B_{\text{T}}(2\text{nd})$ value. Figure 9(b) shows the maximum temperature rise, T_{\max} , of the composite (w/yoke) at $T_{\text{s}} = 20$ K, as a function of second applied pulsed field, $B_{\text{ex}2}(\text{Hall})^{\max}$. T_{\max} for the single pulse application of the composite (w/yoke) at $T_{\text{s}} = 20$ K is also shown, which was presented in figure 7(a). It should be noted that T_{\max} after the second pulse application is about 2 K smaller than that for the single

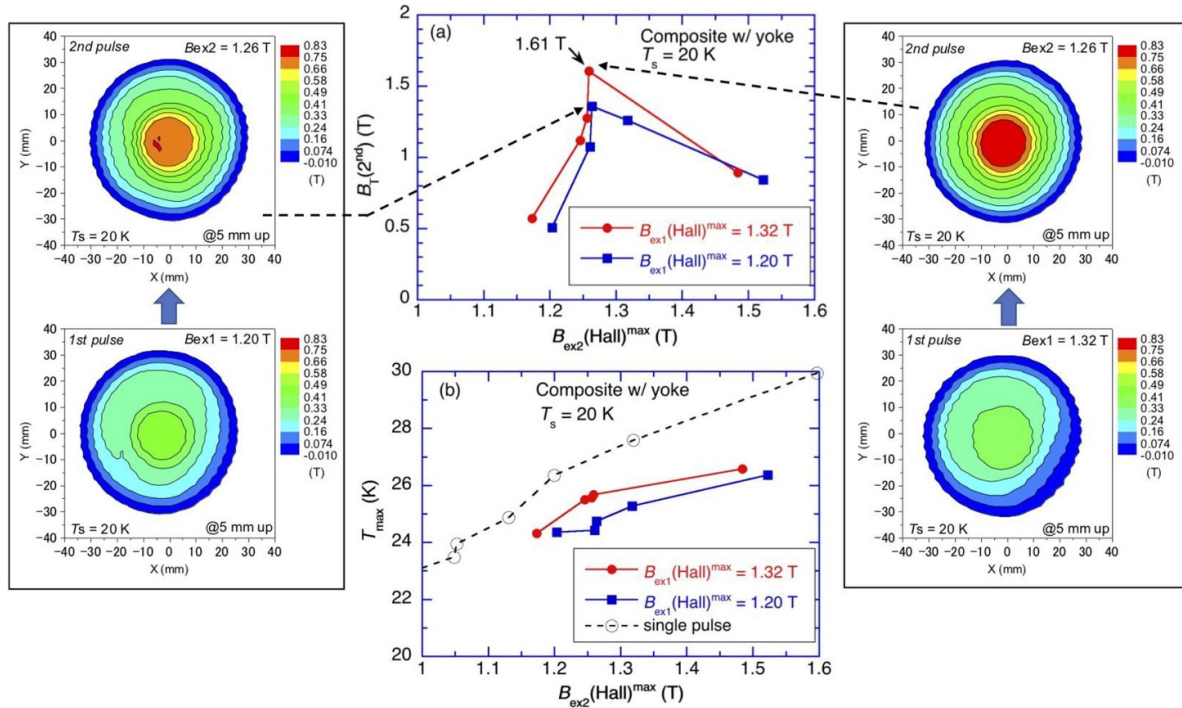


Figure 9. (a) The trapped field, B_T (2nd), on the central surface of the composite (w/yoke) at $T_s = 20$ K, as a function of the second applied pulsed field, $B_{ex2}(\text{Hall})$, after the first pulsed fields, $B_{ex1}(\text{Hall})^{\max}$, of 1.20 T and 1.32 T were applied. The trapped field profiles of the composite (w/yoke) measured 5 mm above the bulk surface at 20 K, for which the maximum B_T (2nd) was achieved for $B_{ex1}(\text{Hall})^{\max} = 1.20$ T and 1.32 T. (b) The maximum temperature rise, T_{\max} , of the composite (w/yoke) at $T_s = 20$ K, as a function of $B_{ex2}(\text{Hall})^{\max}$. T_{\max} for the single pulse application for the composite (w/yoke) at $T_s = 20$ K is also shown.

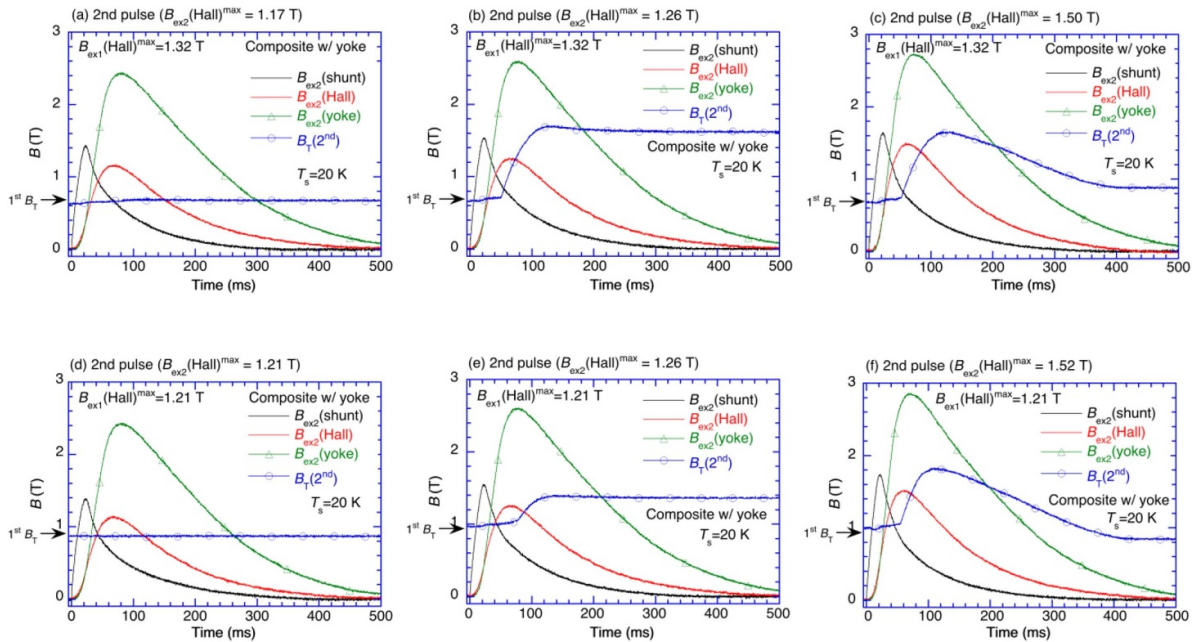


Figure 10. The time dependence of the applied fields, $B_{ex2}(t)$, and the trapped field, $B_T(2nd)(t)$ for the second pulse application, $B_{ex2}(\text{Hall})^{\max}$, after the first pulse application of (a)–(c) $B_{ex1}(\text{Hall})^{\max} = 1.32$ T and (d)–(f) $B_{ex1}(\text{Hall})^{\max} = 1.21$ T at $T_s = 20$ K.

pulse application. The reduction of temperature rise results in the enhancement of B_T after the second pulse.

Figures 10(a)–(c), respectively, show the time dependence of the applied fields, $B_{ex2}(\text{shunt})(t)$, $B_{ex2}(\text{Hall})(t)$ for w/o yoke and $B_{ex2}(\text{yoke})(t)$ for w/yoke, and the trapped field, $B_T(2nd)(t)$,

at $T_s = 20$ K for $B_{ex2}(\text{Hall})^{\max} = 1.17, 1.26$ and 1.50 T, after the first pulse of $B_{ex1}(\text{Hall})^{\max} = 1.32$ T was applied. The time dependence of $B_T(1st)(t)$ for $B_{ex1}(\text{Hall})^{\max} = 1.32$ T was shown in figure 8(i), in which $B_T(1st) = 0.65$ T was trapped. For $B_{ex2}(\text{Hall})^{\max} = 1.26$ T, the maximum $B_T(2nd)$ of 1.61 T

was achieved. Figures 10(d)–(f), respectively, show the time dependence of applied fields and the trapped field, $B_T(2nd)(t)$, at $T_s = 20$ K for $B_{ex2}(\text{Hall})^{\max} = 1.21, 1.26$ and 1.52 T, after the first pulse of $B_{ex1}(\text{Hall})^{\max} = 1.20$ T was applied. The time dependence of $B_T(1st)(t)$ for $B_{ex1}(\text{Hall})^{\max} = 1.21$ T was shown in figure 8(h), in which $B_T(1st) = 1.00$ T was trapped.

As shown in figure 9(a), a similar trend can be seen after the $B_{ex1}(\text{Hall})^{\max}$ application of 1.32 and 1.20 T, although a slight difference in the maximum value of $B_T(2nd)$ exists. However, the $B_T(t)$ behavior was different after the identical $B_{ex2}(\text{Hall})^{\max} = 1.26$ T application, as shown in figures 10(b) and (e). In the case of $B_{ex1}(\text{Hall})^{\max} = 1.32$ T, which was higher than the optimum $B_{ex1}(\text{Hall})^{\max}$ shown in figure 6, $B_T(1st)$ was as low as 0.65 T. For the 2nd pulse application of $B_{ex2}(\text{Hall})^{\max} = 1.26$ T, a clear $B_T(2nd)(t)$ enhancement up to 1.61 T can be observed. On the other hand, in the case of $B_{ex1}(\text{Hall})^{\max} = 1.20$ T, which was the optimum $B_{ex1}(\text{Hall})^{\max}$ shown in figure 6, $B_T(1st)$ was 1.00 T. For the 2nd pulse application of $B_{ex2}(\text{Hall})^{\max} = 1.26$ T, the $B_T(2nd)(t)$ enhancement was relatively small. These results suggest that the enhancement of $B_T(2nd)$ is sensitive to the trapped field profile in the bulk after the 1st pulse application. A similar trend in the enhancement of $B_T(2nd)$ was observed in the results from the MMPSC method for the GdBaCuO bulk in [17].

4. Conclusion

We have investigated the pulsed field magnetization (PFM) of three types of MgB₂ bulk modules (single ring bulk, composite (w/o yoke) and composite (w/yoke)) using a split-type coil (also inserting a soft iron yoke) at $T_s = 20$ K. The composite (w/o yoke) consisted of two MgB₂ ring bulks sandwiched by thin oxygen-free copper ring plates, which were then stacked. The composite (w/yoke) module included a soft iron yoke cylinder that was inserted in the composite (w/o yoke). We also studied the effect of the copper plates and soft iron yoke to enhance the trapped field, B_T . The important results and conclusions are summarized as follows.

- (1) The copper plates delayed the rise time of magnetic pulse due to the flow of the eddy currents. The inserted soft iron yoke attracted the magnetic flux and enhanced the trapped field due to its large permeability. Both parts contribute to the magnitude and shape of the effective pulsed field, B_{ex} .
- (2) The trapped field was enhanced from $B_T = 0.34$ T for the single MgB₂ ring bulk without both the copper plates and soft iron yoke to $B_T = 0.44$ T for the composite (w/o yoke) and, finally to $B_T = 1.00$ T for the composite (w/yoke). The inserted soft iron yoke can be exploited to enhance the trapped field because the intrinsic B_T of the single MgB₂ ring bulk was smaller than the saturation field of the yoke.
- (3) Using the optimized second pulse application after appropriate flux trapped, $B_T(1st)$, by the first pulse, B_{ex1} , the trapped field was enhanced considerably to $B_T(2nd) = 1.61$ T, which is a record-high trapped field for MgB₂ bulk by PFM to date.
- (4) The combination of the longer magnetic pulse by the copper plates, the enhancement of the effective applied field by the inserted soft iron yoke and the double pulse application using the split-type coil is an effective technique to enhance the trapped field in the MgB₂ bulk using PFM. This composite structure with copper plates and an iron yoke may also be applicable to REBaCuO bulk trapped field magnets magnetized by PFM.

Acknowledgments

The authors thank Dr Mark D Ainslie of University of Cambridge for his valuable discussions and suggestions. This research is supported by Adaptable and Seamless Technology transfer Program through Target-driven R&D (A-STEP) from Japan Science and Technology Agency (JST), Grant No. VP30218088419 and by JSPS KAKENHI Grant No. 19K05240.

ORCID iDs

Tatsuya Hirano  <https://orcid.org/0000-0003-1658-914X>
 Sora Namba  <https://orcid.org/0000-0001-7268-5326>
 Tomoyuki Naito  <https://orcid.org/0000-0001-7594-3466>
 Hiroyuki Fujishiro  <https://orcid.org/0000-0003-1483-835X>

References

- [1] Weinstein R, Parks D, Sawh R-P, Carpenter K and Davey K 2016 *J. Appl. Phys.* **119** 133906
- [2] Zou J, Ainslie M D, Fujishiro H, Bhagurkar A G, Naito T, Hari Babu N, Fagnard J-F, Vanderbemden P and Yamamoto A 2015 *Supercond. Sci. Technol.* **28** 075009
- [3] Fujishiro H, Mochizuki H, Naito T, Ainslie M D and Giunchi G 2016 *Supercond. Sci. Technol.* **29** 034006
- [4] Fujishiro H, Tateiwa T, Fujiwara A, Oka T and Hayashi H 2006 *Physica C* **445–8** 334
- [5] Zhou D, Izumi M, Miki M, Felder B, Ida T and Kitano M 2012 *Supercond. Sci. Technol.* **25** 103001
- [6] Bhagurkar A G, Yamamoto A, Anguilano L, Dennis A R, Durrell J H, Hari B N and Cardwell D A 2016 *Supercond. Sci. Technol.* **29** 035008
- [7] Yamamoto A, Ishihara A, Tomita M and Kishio K 2014 *Appl. Phys. Lett.* **105** 032601
- [8] Fujishiro H, Ujiie T, Mochizuki H, Yoshida T and Naito T 2015 *IEEE Trans. Appl. Supercond.* **25** 6800104
- [9] Hirano T, Fujishiro H, Naito T, Ainslie M D and Shi Y-H 2019 *IEEE Trans. Appl. Supercond.* **29** 6801705
- [10] Fujishiro H, Naito T and Oyama M 2011 *Supercond. Sci. Technol.* **24** 075015
- [11] Kambara M, Babu N H, Sadki E S, Cooper J R, Minami H, Cardwell D A, Campbell A M and Inoue I H 2001 *Supercond. Sci. Technol.* **14** L5
- [12] Bhagurkar A G, Yamamoto A, Wang L, Xia M, Dennis A R, Durrell J H, Aljohani T A, Babu N H and Cardwell D A 2018 *Sci. Rep.* **8** 13320
- [13] Fujishiro H, Ujiie T, Naito T, Albisetti A F and Giunchi G 2014 *J. Phys.: Conf. Ser.* **507** 032016
- [14] Naito T, Yoshida T and Fujishiro H 2015 *Supercond. Sci. Technol.* **28** 095009
- [15] Huang K Y *et al* 2020 *Supercond. Sci. Technol.* **33** 02LT01

- [16] Hayashi H, Tsutsumi K, Saho N, Nishijima N and Asano K 2003 *Physica C* **392–6** 745–8
- [17] Zhou D, Shi Y-H, Dennis A R, Cardwell D A and Durrell J H 2020 *Supercond. Sci. Technol.* **33** 034001
- [18] Fujishiro H, Tamura T, Arayashiki T, Oyama M, Sasaki T, Naito T, Giunchi G and Albisetti A F 2012 *Jpn. J. Appl. Phys.* **51** 103005
- [19] Nakamura T, Tamada D, Yanagi Y, Itoh Y, Nemoto T, Utumi H and Kose K 2015 *J. Magn. Reson.* **259** 68–75
- [20] Oka T et al 2019 *IEEE Trans. Appl. Supercond.* **29** 6802606
- [21] Zhou D, Ainslie M D, Srpcić J, Huang K-Y, Shi Y-H, Dennis A R, Cardwell D A, Durrell J H, Boll M and Filipenko M 2018 *Supercond. Sci. Technol.* **31** 105005
- [22] Fujishiro H, Tateiwa T, Kakehata K, Hiyama T and Naito T 2007 *Supercond. Sci. Technol.* **20** 1009–14
- [23] Gotoh S, Murakami M, Fujimoto H and Koshizuka N 1992 *J. Appl. Phys.* **72** 2404–10
- [24] Ainslie M D, Fujishiro H, Ujiie T, Zou J, Dennis A R, Shi Y-H and Cardwell D A 2014 *Supercond. Sci. Technol.* **27** 065008
- [25] Werfel F N, Floegel-Delor U, Rothfeld R, Riedel T, Goebel B, Wippich D and Schirrmeister P 2012 *Supercond. Sci. Technol.* **25** 014007
- [26] Fuchs G, Häbler W, Nenkov K, Scheiter J, Perner O, Handstein A, Kanai T, Schultz L and Holzapfel B 2013 *Supercond. Sci. Technol.* **26** 122002
- [27] Ikuta H, Ishihara H, Yanagi Y, Itoh Y and Mizutani U 2002 *Supercond. Sci. Technol.* **15** 606
- [28] Durrell J H et al 2014 *Supercond. Sci. Technol.* **27** 082001
- [29] Miyazaki T, Fukui S, Ogawa J, Sato T, Oka T, Scheiter J, Hasler W, Kulawansha E, Yuanding Z and Yokoyama K 2017 *IEEE Trans. Appl. Supercond.* **27** 6800504
- [30] Ida T et al 2004 *Physica C* **412–4** 638–45
- [31] Fujishiro H, Hiyama T, Miura T, Naito T, Nariki S, Sakai N and Hirabayashi I 2009 *IEEE Trans. Appl. Supercond.* **19** 3545–8
- [32] Ainslie M D, Zhou D, Fujishiro H, Takahashi K, Cardwell D A and Durrell J H 2018 *IEEE Trans. Appl. Supercond.* **28** 6800207
- [33] Ogino A, Naito T and Fujishiro H 2017 *IEEE Trans. Appl. Supercond.* **27** 6800905
- [34] Sander M, Sutter U, Koch R and Klaser M 2000 *Supercond. Sci. Technol.* **13** 841
- [35] Fujishiro H, Kaneyama M, Yokoyama K, Oka T and Noto K 2005 *Jpn. J. Appl. Phys.* **44** 4919–25
- [36] Durrell J H, Dancer C E J, Dennis A, Shi Y, Xu Z, Campbell A M, Hari N, Todd R I, Grovenor C R M and Cardwell D A 2012 *Supercond. Sci. Technol.* **25** 112002
- [37] Ainslie M D, Fujishiro H, Mochizuki H, Takahashi K, Shi Y-H, Namburi D K, Zou J, Zhou D, Dennis A R and Cardwell D A 2016 *Supercond. Sci. Technol.* **29** 074003
- [38] Ogawa K, Nakamura T, Terada Y, Kose K and Haishi T 2011 *Appl. Phys. Lett.* **98** 234101
- [39] Fujishiro H, Mochizuki H, Ainslie M D and Naito T 2016 *Supercond. Sci. Technol.* **29** 084001
- [40] Yanagi Y, Itoh Y, Yoshikawa M, Oka T, Hosokawa T, Ishihara H, Ikuta H and Mizutani U 2000 *Advances in Superconductivity* vol 12 (Tokyo: Springer) pp 470